

TCAD simulations of irradiated power diodes over a wide temperature range

Marco Bellini

ABB Corporate Research,
Dattwil, Switzerland
e-mail: marco.bellini@ch.abb.com

Jan Vobecký*

ABB Switzerland Ltd, Semiconductors,
Lenzburg, Switzerland

Abstract—A SRH model with temperature-dependent capture cross-sections is proposed for a better accuracy of TCAD simulations of combined ion and electron irradiated power diodes over a large temperature range. A robust procedure is proposed for the identification of the model parameters of deep levels on the basis of static and dynamic diode measurements.

Keywords—component; TCAD; power diodes; trap models

I. INTRODUCTION

The optimal trade-off between on-state and switching losses in power semiconductor devices such as diodes, IGBTs, and thyristors is reached through lifetime control. Irradiation techniques are superior to other methods like diffusion of transition metals, because they are easier to apply and their controllability and reproducibility is much higher. Irradiation with electrons, protons or alpha particles is used to selectively shape the lifetime across the depth of the device. This way, the plasma distribution prior to turn-off is shaped to give optimal turn-off parameters. Since power devices operate in a wide range of temperatures, in which the electronic parameters of the plurality of deep levels introduced by the irradiation change significantly, electro-thermal device simulation with calibrated models of deep level parameters is needed [1]. TCAD models of deep level parameters efficiently calibrated in a wide range of temperatures can reduce significantly the time and cost of development of improved power devices.

This work introduces two improvements in the state-of-the-art of simulations of irradiated devices. First, the temperature dependence of capture cross-sections is incorporated in the Sentaurus Device simulator [2]. Then, an efficient calibration scheme, based on simple, routine device measurements is presented. The calibration routine ensures that the parameters have physically meaningful values compared to literature. These improvements are demonstrated in this paper on power diodes irradiated with electrons and helium ions, but they can be applied to a variety of power devices and deep levels. Furthermore, the optimization techniques described in this work can be applied to a large number of TCAD problems such as model fitting or device performance improvement to reach the optimal trade-off of several figures of merit.

II. IMPROVED MODEL OF CAPTURE CROSS-SECTIONS

The models implemented in most commercial device simulators allow only deep levels with constant cross-sections σ with respect to temperature [2], in contrast with the findings of [3][4][5]. Since silicon power semiconductor devices operate typically between -40 °C and $+180$ °C, the use of constant cross-sections can lead to errors of up to 30% in the capture and emission rates across the temperature range.

The mathematical implementation of the improved model in the Sentaurus Device simulator is straightforward. The occupation model of a deep level is based on the electron c_C^n capture rate from the conduction band, the hole capture rate from the valence band c_V^p , the electron emission rate to the conduction band e_C^n and the hole emission rate to the valence band e_V^p . The capture and emission rate for the electrons can be expressed as:

$$c_C^n = \sigma_n v_{th} n, \quad e_C^n = \sigma_n v_{th} n_1 \quad (1)$$

where n is the electron concentration, and v_{th} is the thermal velocity. In the standard Sentaurus implementation the cross-sections σ_n and σ_p are constant with temperature. The excess electron concentration n_1 is described by:

$$n_1 = n_{i,eff} \exp\left(\frac{-E_{trap,Midgap}}{kT}\right) \quad (2)$$

which depends on the distance of the trap from the middle of the bandgap and on the effective density of states $n_{i,eff}$. Similar equations can be written for the holes. The temperature dependence of $n_{i,eff}$ is taken into account with:

$$n_{i,eff} = \sqrt{N_C N_V} \exp\left(\frac{-E_{g,eff}}{2kT}\right) \quad (3)$$

where N_V and N_C indicate the effective density of states for the valence and the conduction band and $E_{g,eff}$ is the effective bandgap (accounting for the effects of bandgap narrowing). The temperature dependence of N_V and N_C is modeled by:

$$N_V = 2.5094e-19 \left(\frac{m_p}{m_0} \right)^{3/2} \left(\frac{T_p}{300} \right)^{3/2} \quad (4)$$

$$N_C = 2.5094e-19 \left(\frac{m_n}{m_0} \right)^{3/2} \left(\frac{T_n}{300} \right)^{3/2} \quad (5)$$

where and T_n and T_p are the electron and hole temperatures and m_p and m_n are the hole and electron effective masses. Furthermore the effective mass for the holes m_p and the longitudinal m_l and transversal m_t components of the effective mass for the electrons m_n are expressed by:

$$m_n = 6^{2/3} (m_l m_t)^{1/3} + m_m \quad (6)$$

$$\frac{m_t(T)}{m_0} = a_t \frac{E_g(0)}{E_g(T)} \quad (7)$$

$$\frac{m_p(T)}{m_0} = \left(\frac{a + bT + cT^2 + dT^3 + eT^4}{1 + fT + gT^2 + hT^3 + iT^4} \right)^{2/3} + m_m \quad (8)$$

where $E_g(0)$ is the energy bandgap at 300 K and $E_g(T)$ describes the energy bandgap as a function of temperature (without accounting for bandgap narrowing). The remaining constants are described in the works of [6] and [7]. Finally, both the Bennett and Slotboom bandgap narrowing models are implemented.

The conventional model is extended by introducing capture cross-sections with an exponential and power law dependence on temperature, as suggested in [3][4][5]:

$$c_C^n = \sigma_0 \exp(-T/T_a) v_{th} n \quad (9)$$

$$c_C^n = \sigma_0 (T^{T_a}) v_{th} n \quad (10)$$

The Sentaurus Device simulator offers two possibilities for the numerical implementation of the equations. The “simplified C++ interface” requires only the implementation of the equations (1)-(10). The derivatives of the trap rates with respect to the unknowns – used to evaluate the Jacobian matrix – are evaluated numerically. However this approach does not achieve the best computation speed and convergence properties. Therefore, it’s recommended to use the standard “standard C++ interface” which requires the implementation of the mathematical derivatives of the electron and hole capture and emission rates. Given the complexity of (1)-(10) it’s not advised to calculate manually the derivatives of the rates. In fact the C++ routine for the derivatives with respect to temperature comprises several hundreds lines of code. To simplify the coding of the model and to avoid possible implementation errors it’s best to use a computer algebra system such as Maxima, MATLAB or Mathematica to compute the symbolic derivatives and translate automatically the mathematical expressions to C++. This procedure allows to quickly extend the model, introducing additional cross-section functional dependencies if needed.

III. MODEL CALIBRATION PROCEDURE

Calibrating a TCAD model is often a very challenging task if many parameters are available and considerable accuracy over several characteristics is required. This problem is exacerbated, if the range of some parameters is not known with sufficient precision, as in the case of the capture cross-sections.

Consequently the model calibration procedure requires a sequence of steps. First, the device mesh is initialized with accurate representations of the doping, and of the electron and He deep level densities. Then, basic recombination parameters are extracted for the unirradiated device. Subsequently, the circuit used for the simulation of the reverse recovery is adjusted to obtain the same di/dt . Finally, a complex multi-objective optimization procedure is used to ensure accurate reproduction of static characteristics and reverse recovery.

A. Device-under-test and measured data

The devices examined in this paper are irradiated with 1 - 5 MeV electrons at a dose between 5 and 20 kGy and 5 - 12 MeV He at doses ranging between $1 \cdot 10^{10} - 1 \cdot 10^{11} \text{ cm}^{-2}$ and annealed at a temperature below 300°C. In these conditions the dominant deep levels are the vacancy-oxygen pair (V-O) at $\approx E_C - 0.16 \text{ eV}$ and the divacancy (V-V) at $\approx E_C - 0.42 \text{ eV}$ [3].

The diodes’ DC characteristics, measured at temperatures of 80 °C, 125 °C, and 140 °C and at currents of 1 kA, 2kA, 3kA, and 4kA, are shown in Fig. 1, along with the simulations resulting from the optimization procedure presented in this work.

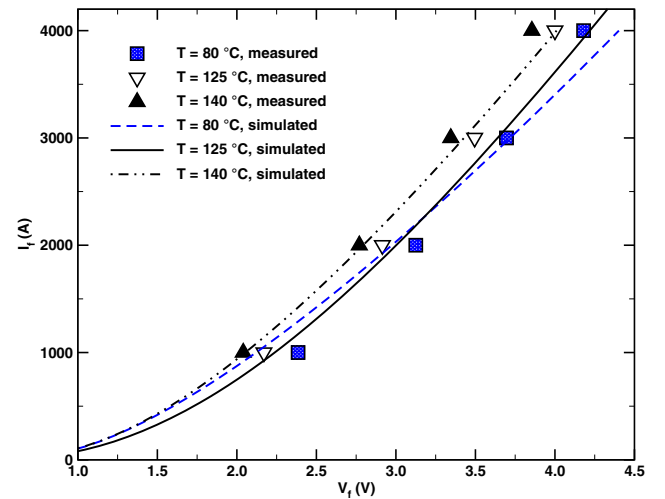


Figure 1. Measured and simulated DC characteristics $I_f - V_f$ at temperatures of 80 °C, 125 °C, and 140 °C.

In any TCAD simulation, robust parameter fitting procedures are needed to advance from qualitative to quantitative agreement with measured data. This is especially true in the case of capture cross-sections, because the model values found in literature are usually measured through the DLTS technique at cryogenic temperatures and extrapolated to room temperature [4]. In some cases, optical and electrical measurements of carrier lifetime at room temperature such as

OCCD and OCVD [3][4][5], resp. can be employed to mitigate the uncertainty of the model parameters. However, these techniques cannot be used for any device since they are based either on optical carrier generation or they give only an effective value of lifetime. Conversely, the fitting procedure proposed here is based only on the measurements of DC characteristics and reverse recovery waveforms which are standard testing procedures for power diodes.

B. Model initialization and preliminary operations

First a 1D diode mesh is created using doping profiles measured by the spreading resistance method. The diode forward characteristics at several temperatures (40 °C, 80 °C, 125 °C, and 140 °C) are calibrated by adjusting the SRH and Auger coefficients. Then, the trap profiles created by ions and electrons are simulated with the SRIM [8] and CASINO [9] software and introduced in the mesh file. Subsequently, the measured forward characteristics $I_f - V_f$ are fitted for different temperatures after He irradiation. Then, the measured $I_f - V_f$ are fitted after both He and electron irradiation, to provide an initial guess for the multi-objective algorithm. The schematic of testing circuit used for reverse recovery measurements is shown in Fig 2. The exact value of the inductance LS used in the test is fine-tuned to match the dI/dt of the measurements. The measured reverse recovery current at temperatures of 80 °C, 125 °C, and 140 °C is shown in Fig. 3, along with the simulated characteristics.

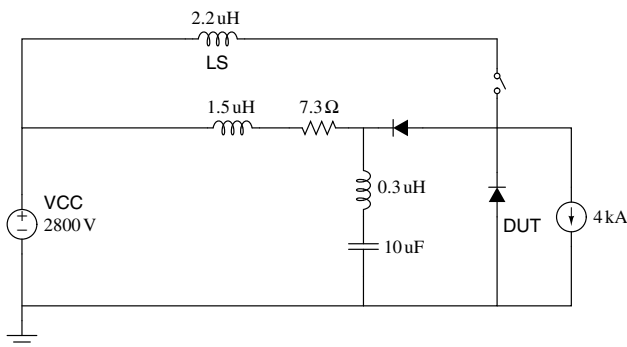


Figure 2. Circuit used for reverse recovery simulations.

C. Multi-objective model fitting

As mentioned in [10], simply fitting the forward characteristics does not ensure sufficient accuracy in simulating the reverse recovery. Conversely, reproducing accurately both static and dynamic curves means that the spatial distribution of the deep levels and their behavior at the low and high injection are precisely modeled. In addition to the cross-sections of deep levels, also the impact ionization coefficients must also be fitted to obtain agreement between the simulated and measured reverse recovery waveforms at the time of fast growing reverse voltage (dynamic avalanche). This results in an optimization problem with dimensionality between 5 and 12, according to how many variables are considered. Each variable is typically explored in a span of 2 decades around its typical value. Unfortunately, simulations of the reverse recovery of diodes with large amounts of deep levels and realistic circuits are

notoriously slow due to the poor convergence rate, limiting the number of function evaluations that the optimization algorithm is able to use in a practical application.

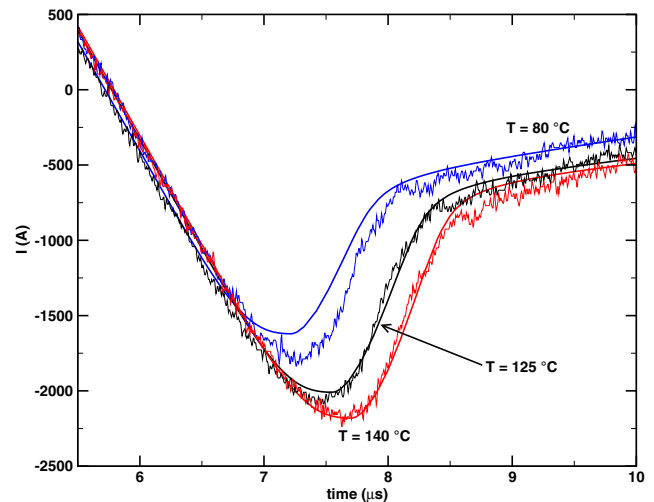


Figure 3. Measured and simulated reverse recovery characteristics at temperatures of 80 °C, 125 °C, and 140 °C

Therefore, the proper multi-objective algorithm must be chosen to achieve accurate fitting of DC and reverse recovery in a large parameter space using very few TCAD simulations. In order to avoid local minima, popular but unsophisticated techniques like the simplex method cannot be used. A better choice is the high-performance, single objective Covariance Matrix Adaptation Evolution Strategy (CMA-ES) algorithm [11]. The use a maximum likelihood optimizer and the ability to continuously update the covariance matrix of the candidate parameter distribution and to control the step size with a genetic evolution strategy enable CMA-ES to quickly solve difficult optimization tasks such as the fitting of the diode DC characteristics. However, CMA-ES does not provide optimal performance for the simultaneous optimization of reverse recovery and $I_f - V_f$. To use CMA-ES the errors in the two simulations must be combined in a single figure of merit. This can be done with a linear combination but it's very difficult to decide *a priori* the optimal weights. In alternative, the product of the two errors can be minimized. This approach produces the plot of Fig 4, showing the tradeoff between the accuracy of the DC characteristic versus the accuracy of the reverse recovery. Each dot is produced by a simulation with a particular choice of the parameters. The crosses indicate the parameter values, found by CMA-ES, which minimize the product of the two errors. As shown, these values emphasize excessively the accuracy of the transient simulation at the expense of the DC simulation. The plot also clearly shows a numerical approximation of the Pareto Frontier – a line representing the best tradeoff between the two errors. Once the Pareto Frontier is individuated, the selection of the best parameters is straightforward. However, there is no guarantee that CMA-ES, optimizing the product of the errors, will get close enough to the Pareto Frontier or even identify it fully, as shown in Fig. 4. To overcome these issues, the NSGA-II genetic algorithm is used [12]. NSGA-II enforces population selection with elitism for dominant solutions, guaranteeing a

robust individuation of the Pareto Frontier and convergence to better solutions.

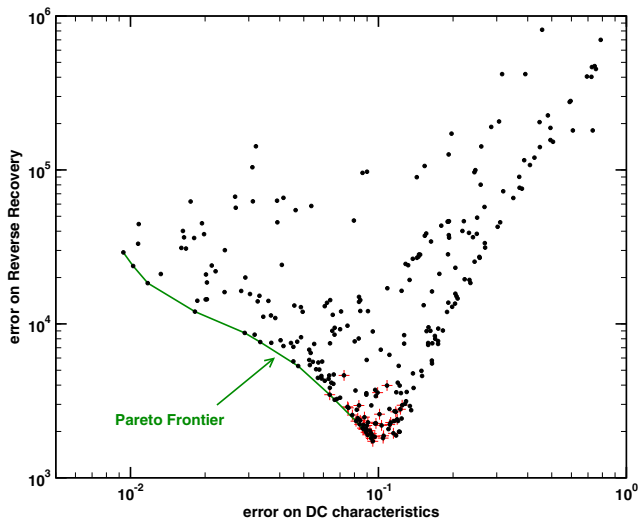


Figure 4. Plot of the error in the fitting of the DC characteristics versus the error in the reverse recovery.

D. Discussion of the results

The fitting of DC characteristics and reverse recovery for various temperatures is shown in Fig. 1 and 2. The NSGA-II algorithm converges to a quite accurate solution in a few hours for each temperature point.

The proposed trap model also allows plotting the contribution of every deep level to the overall recombination-generation rate during device operation, as shown in Fig. 5.

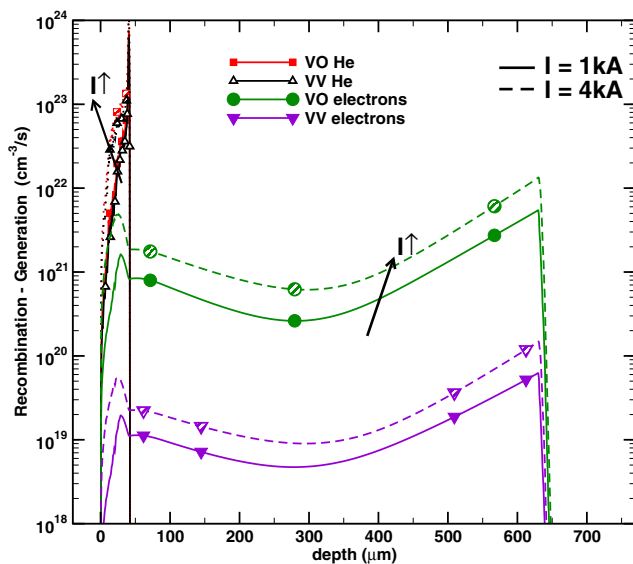


Figure 5. Trap contributions to total R-G rate at $T = 40\text{ }^{\circ}\text{C}$.

Simulations demonstrate that at high injection the temperature dependence of the cross-section strongly influences recombination and lifetime. Conversely, at low level injection the excess carrier concentrations also play a significant role in accord with [3].

IV. CONCLUSIONS

The accuracy of TCAD simulations of power devices over a wide temperature range is increased by implementing a model with temperature-dependent cross-sections of deep levels. Also, a robust parameter extraction procedure based on standard device test measurements and able to provide physically meaningful parameter values, is proposed. Finally, the new model can be used to visualize the contribution of each trap level to the overall recombination-generation rate during device operation, assisting the design of the optimal lifetime profile.

REFERENCES

- [1] J. Vobecky, P. Hazdra, O. Humbel, and N. Galster, "Crossing point current of electron and proton irradiated power P-i-N diodes," *Microelectronics Reliability*, vol. 40, 2000, pp. 427-433.
- [2] Sentaurus Device User Guide, Version *D-2010.03*, Synopsys, 2010.
- [3] R. Siemieniec, W. Sudkamp, and J. Lutz, "Determination of parameters of radiation induced traps in silicon," *Solid-State Electronics*, vol. 46, 2002, pp. 891-901.
- [4] R. Siemieniec, F.-J. Niedernostheide, F.-J. Schulze, W. Südkamp, and J. Kellner-Werdehausen, W. Lutz, "Irradiation-Induced Deep Levels In Silicon" *Proc. 206th Annual Meeting of ECS*, 2004.
- [5] H. Bleichner, P. Jonsson, N. Keskitalo, and E. Nordlander, "Temperature and injection dependence of the Shockley-Read-Hall lifetime in electron irradiated n-type silicon," *Journal of Applied Physics*, vol. 79, 1996, pp. 9142-9148.
- [6] M.A. Green, "Intrinsic concentration, effective densities of states, and effective mass in silicon," *Journal of Applied Physics*, vol. 67, 1990, pp. 2944-2954.
- [7] J. E. Lang, F. L. Madarasz, and P. M. Hemenger, "Temperature dependent density of states effective mass in nonparabolic p-type silicon," *Journal of Applied Physics*, vol. 54, no. 6, 1983, p. 3612
- [8] J. F. Ziegler, and J. M. Manoyan, "The stopping of ions in compounds," *Nuclear Instruments and Methods in Physics Research Section B: Beam Interactions with Materials and Atoms*, vol. 35, 1988, pp. 215-228.
- [9] R.J. Needs, M.D. Towler, N.D. Drummond, and P. López Ríos, "Continuum variational and diffusion quantum Monte Carlo calculations," *Journal of Physics: Condensed Matter*, vol. 22, Jan. 2010, p. 023201.
- [10] F. Cappelluti, F. Bonani, M. Furno, G. Ghione, R. Carta, L. Bellemo, C. Bocchiola, and L. Merlin, "Physics-based mixed-mode reverse recovery modeling and optimization of Si PiN and MPS fast recovery diodes," *Microelectronics Journal*, vol. 37, Mar. 2006, pp. 190-196.
- [11] N. Hansen and R. Ros, "Benchmarking a weighted negative covariance matrix update on the BBOB-2010 noisy testbed," *Proceedings of the 12th annual conference comp on Genetic and evolutionary computation*, ACM, 2010, pp. 1681-1688.
- [12] Deb, K., A. Pratap, S. Agarwal, and T. Meyarivan. 2002. "A fast and elitist multiobjective genetic algorithm: NSGA-II," *IEEE Transactions on Evolutionary Computation*, vol. 6, no. 2, pp. 182-197.